The 95F Unconventional Myosin Is Required for Proper Organization of the *Drosophila* Syncytial Blastoderm

Valerie Mermall and Kathryn G. Miller

Department of Biology, Washington University, St. Louis, Missouri 63130

Abstract. The 95F myosin, a class VI unconventional myosin, associates with particles in the cytoplasm of the *Drosophila* syncytial blastoderm and is required for the ATP- and F-actin–dependent translocation of these particles. The particles undergo a cell cycle–dependent redistribution from domains that surround each nucleus in interphase to transient membrane invaginations that provide a barrier between adjacent spindles during mitosis. When 95F myosin function is inhibited by antibody injection, profound defects in syncytial blastoderm organization occur. This disorganization is seen as aberrant nuclear morphology and position and is suggestive of failures in cytoskeletal function. Nuclear defects correlate with gross defects in the actin cytoskeleton, including indistinct actin caps and furrows, missing actin structures, abnormal spacing of caps, and abnormally spaced furrows. Three-dimensional examination of embryos injected with anti–95F myosin antibody reveals that actin furrows do not invaginate as deeply into the embryo as do normal furrows. These furrows do not separate adjacent mitoses, since microtubules cross over them. These inappropriate microtubule interactions lead to aberrant nuclear divisions and to the nuclear defects observed. We propose that 95F myosin function is required to generate normal actin-based transient membrane furrows. The motor activity of 95F myosin itself and/or components within the particles transported to the furrows by 95F myosin may be required for normal furrows to form.

MYOSINS are mechanochemical enzymes that use the energy of ATP hydrolysis to generate force and are the only known actin-based motors. The myosins form a large, diverse family of proteins with two major subdivisions, the conventional and unconventional myosins. The conventional myosins are all structurally similar to those found in muscle. The F-actin–binding, ATP hydrolysis, and actin translocation activities reside in the head domain; dimerization and the formation of bipolar filaments are mediated through the tail domain. These myosins are responsible for the actin-based movements of muscle contraction (Huxley, 1969), receptor capping (Pasternak et al., 1989), and cytokinesis (DeLozanne and Spudich, 1987; Knecht and Loomis, 1987; Karess et al., 1991).

The unconventional myosins are highly variable in structure. At least eight distinct classes of unconventional myosins have been identified (Bement and Mooseker, 1993). Some, such as myosin V, form dimers, but not bipolar filaments (Cheney et al., 1993*a*); others, such as the myosin I molecules, have a single head and short tails (Cheney and Mooseker, 1992). Because of the diversity in tail sequences, the unconventional myosins are thought to mediate many different actin-based dynamic processes.

Address all correspondence to K. G. Miller, Washington University, Campus Box 1229, One Brookings Drive, St. Louis, MO 63130-4899. Tel.: (314) 935-7305 Fax: (314) 935-5125.

The unconventional myosin head domains are related in predicted amino acid sequence to the conventional myosin head domains (Cheney and Mooseker, 1992). As might be expected based on this sequence conservation, the enzymatic properties of the unconventional myosins are similar to those of the conventional myosins; they have actin-activated ATPase activity and ATP-sensitive actin-binding activity and can translocate along actin filaments in vitro (for review of myosin I molecules, see Pollard et al., 1991; for myosin V, see Cheney et al., 1993*a*). Thus, it is thought that they participate in some cell dynamics via translocation on actin. Since *Dictyostelium* mutants in which the conventional myosin II is missing or altered are still capable of many actin-based processes, including translocation, unconventional myosins are thought to be involved in these processes (DeLozanne and Spudich, 1987; Knecht and Loomis, 1987; Peters et al., 1988; Wessels et al., 1988, 1991; Titus et al., 1993). However, the function of individual members of the unconventional myosin group in vivo is in most cases unknown. One exception is *Acanthamoeba* myosin IC, which is required for the proper function of the contractile vacuole, although the precise role of this myosin in contractile vacuole function is unknown (Doberstein et al., 1993). For most unconventional myosins, determining their particular functions in cells remains a major challenge in the field.

One of the postulated functions of the unconventional myosins is cytoplasmic transport of vesicles along actin fil-

aments. We have shown that the *Drosophila* 95F unconventional myosin (class VI) drives the movement of particles in the cytoplasm of living embryos (Mermall et al., 1994), demonstrating that at least one unconventional myosin participates in transport in vivo. Localization studies in a variety of cell types (Fukui et al., 1989; Baines et al., 1992; Wagner et al., 1992), cell fractionation data (Adams and Pollard, 1986; Miyata et al., 1989; Fath and Burgess, 1993; Fath et al., 1994), and biochemical studies (Zot et al., 1992) provide indirect evidence that participation in transport may be a widespread property of the unconventional myosins. In addition, unconventional myosin-mediated transport of vesicles has been demonstrated in vitro (Adams and Pollard, 1986).

Our studies focus on the role of the *Drosophila* 95F unconventional myosin during development. 95F myosin is the founding member of class VI (Kellerman and Miller, 1992; Cheney et al., 1993*b*). This myosin class is likely to be ubiquitous, since it is found in widely diverse species, such as pig and nematode in addition to *Drosophila* (Kellerman and Miller, 1992; Bement et al., 1994; Hasson and Mooseker, 1994; and M. Titus, personal communication). 95F myosin associates with cytoplasmic particles in *Drosophila* embryos (Kellerman and Miller, 1992) and translocates them in a cell cycle–dependent fashion (Mermall et al., 1994). The particles, present throughout the cytoplasmic domain surrounding each syncytial nucleus during interphase, redistribute to transient membrane invaginations often referred to as pseudocleavage or metaphase furrows, during mitosis. The change in 95F myosin distribution led us to investigate further the role of 95F myosin–mediated transport in the actin-based dynamic processes of the early *Drosophila* embryo.

During the syncytial stage of embryonic development, several thousand nuclei form a monolayer in the cortical cytoplasm beneath the plasma membrane and undergo several rounds of very rapid, nearly synchronous division. Actin-based cytoplasmic organization is required to maintain the fidelity of nuclear divisions in the syncytium (Zalokar and Erk, 1976). Actin-based metaphase furrows form between adjacent mitoses (Fig. 1) and are required to maintain separation of neighboring mitotic spindles (Postner et al., 1992; Sullivan et al., 1993*b*). Actin undergoes a dramatic redistribution from metaphase furrows to interphase caps (Fig. 1), which are important for the maintenance of the relative position of syncytial nuclei (Postner et al., 1992). The maintenance of nuclear position is critical as nuclei respond to positional information in the embryo before cellularization occurs (Hafen et al., 1984). We find that 95F myosin function is required for normal actin-based structures to form. Inhibition of 95F myosin function leads to dramatic defects in syncytial blastoderm organization, suggesting that this myosin plays an important role in *Drosophila* development.

Materials and Methods

Fly Culture

Oregon R wild-type flies were maintained at 25°C on yeasted corn meal agar medium. Embryos were collected from yeasted grape juice agar plates.

Microinjections

Embryos were prepared for injection by standard techniques (Ashburner, 1989) and microinjected with control antibody (affinity-purified rabbit polyclonal antibody against glutathione-S-transferase [GST][1] [8–13 mg/ml, final concentration ~80–260 μg/ml] or affinity-purified rabbit polyclonal antibody against 95F myosin heavy chain (Kellerman and Miller, 1992; Mermall et al., 1994) (9–12 mg/ml, final concentration ~90–240 μg/ml). Approximately 1–2% of egg volume was injected. After injection, embryos were incubated in a humidified chamber for 15–30 min before fixation. Embryos were then processed for fluorescence microscopy as will be described. In some experiments, injected antibodies were localized by incubating fixed embryos with FITC-labeled goat anti-rabbit secondary antibodies (Organon Teknika, Durham, NC).

Characterization of Anti–95F Myosin Polyclonal Antibody

Anti–95F myosin polyclonal antibody was affinity purified by transferring bacterially expressed full-length 95F myosin from SDS–polyacrylamide gels to nitrocellulose. The region of the nitrocellulose that contained the 95F myosin was cut out and blocked with 1% BSA in 20 mM Tris, 0.5 M NaCl, 0.05% Tween-20, pH 7.5. Anti–95F myosin rabbit serum was diluted 1:1 and incubated with the membrane overnight at 4°C. The membrane was then washed with TBS (20 mM Tris, 0.5 M NaCl, pH 7.5) and eluted with 100 mM glycine, pH 2.8. The eluted antibody was immediately neutralized with Tris, dialyzed against TBS or PBS, and concentrated with a Centricon ultrafiltration device (Amicon Corp., Danvers, MA).

Anti–95F myosin mAb 3C7 was bound to protein A agarose beads (Bio Rad Laboratories, Richmond, CA) by incubating 900 μl of 3C7 culture supernatant, 100 μl of 500 mM sodium borate, and 100 μl of 5 M NaCl with 25 μl of beads overnight at 4°C and then washed with IP buffer (20 mM Hepes, 150 mM NaCl, 250 mM sucrose, 0.5 mM EDTA, 0.5 mM EGTA, pH 7.5). 95F myosin was bound by incubating these anti–95F myosin antibody beads with 1 ml of clarified extract prepared from 0.5 g of 0–3 h *Drosophila* embryos in 6 ml of IP buffer, 1 mM PMSF overnight at 4°C and then washed with IP buffer plus 350 mM KCl. To assess the effect of

1. *Abbreviations used in this paper*: DAPI, 4,6-diamidino-2-phenylindol; GST, glutathione-S-transferase.

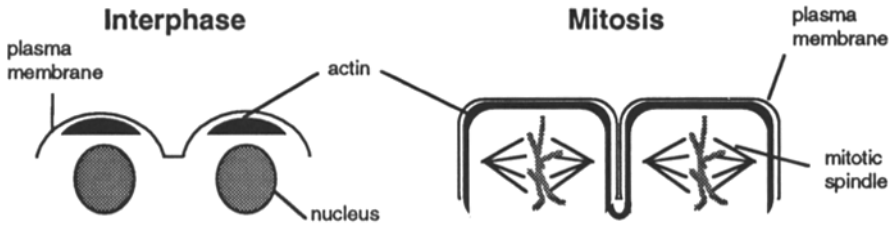

Figure 1. Schematic cross section showing the distribution of F-actin during interphase and mitosis in the syncytial blastoderm *Drosophila* embryo. During interphase, F-actin is concentrated in caps above each nucleus. In mitosis, actin is evenly distributed under the plasma membrane, including the regions between caps where little F-actin is found during interphase. Actin-based metaphase furrows form in these regions and maintain the separation between adjacent mitotic spindles.

anti–95F myosin polyclonal antibody on actin binding, an excess (1.8 μM) of polyclonal antibody or an equal volume of TBS was incubated with the beads for 5 min. F-actin (final concentration 9 μM) stabilized with 10 μg/ml phalloidin was then added to the beads, which were incubated on ice for 30 min. The beads were spun through a step gradient consisting of 500 μl of 30% sucrose and 100 μl of 60% sucrose in IP buffer. Proteins pelleted with the beads were fractionated by SDS-PAGE and stained with Coomassie blue. The relative amounts of actin and 95F myosin that pelleted with the beads were determined by scanning gels with a ScanJet Plus (Hewlett-Packard Co., Palo Alto, CA) or ScanMaker (Microtek International, Inc., Hsinchu, Taiwan, ROC) scanner. The scanned gels were plotted and peak areas were calculated using NIH Image software. To control for slight differences in amounts of protein in each lane, the amount of pelleted actin was normalized for the amount of pelleted 95F myosin within each experiment. These experiments were previously reported in abbreviated form by Mermall et al. (1994).

Fluorescence Labeling and Microscopy

Drosophila embryos were harvested from grape juice plates, dechorionated as previously described (Miller et al., 1989), and fixed in a 2:2:1 mixture of 100 mM Pipes, 1 mM EGTA, 1 mM $MgCl_2$, pH 6.9/heptane/formalin for 25 min, followed by manual devitellinization. Embryos were blocked in 1% BSA in PBS for at least 1 h. Fixed embryos were incubated with rhodamine- or FITC-labeled phalloidin (Sigma Chemical Co., St. Louis, MO) to visualize F-actin and with 4,6-diamidino-2-phenylindol (DAPI; Molecular Probes, Inc., Eugene, OR) to label DNA. 95F myosin was localized by incubation with purified mouse mAb 3C7 (Miller et al., 1989), followed by FITC-labeled goat anti-mouse secondary antibody (Organon Teknika). To visualize tubulin, embryos were fixed as described by Karr and Alberts (1986), except that twice the formalin and 80% of the taxol were used. We found that this fixation method provided optimal fixation of both F-actin and microtubules in injected embryos with a minimum of artifact. Kellogg et al. (1988) found that taxol treatment induced the proliferation of microtubules in the centrosome region and astral microtubules during interphase and prophase. We found minimal taxol-induced artifacts at the reduced concentration of taxol used, and these were most frequently observed in interphase embryos, which were not under consideration in this study. Anti-tubulin mAb (gift of Dr. Bruce M. Alberts, UCSF) and rhodamine-labeled goat anti-mouse antibody (Cappell Laboratories, Malvern, PA) were used to stain tubulin. In some experiments, the plasma membrane was visualized with FITC-labeled Con A (Molecular Probes, Inc.).

Examination of tubulin and actin in three dimensions was performed by computational optical sectioning microscopy (Agard et al., 1989). 64 optical sections, 0.5 μm apart, were collected, and the fluorescence intensity of each focal plane was normalized within the three-dimensional stack of images before processing with a full three-dimensional nonlinear deconvolution method (Joshi and Miller, 1993). Optical sectioning microscopy was also used to produce three-dimensional images of Con A–, phalloidin-, and DAPI-stained embryos. 40 sections were collected 0.5 μm apart and processed as previously described.

Scoring of Defects

The nuclear cycle of fixed embryos was determined by examining DAPI staining to assess nuclear density (Foe and Alberts, 1983). Most embryos were staged by eye; however, DAPI-stained embryos of questionable age were photographed and nuclear density was determined. Embryos fixed in nuclear cycles 12 and 13 were then examined for defects. Injected embryos stained for actin, DNA, and the injected antibody were scanned at 200× for the presence of gross morphological defects in nuclear morphology or in the actin cytoskeleton. A defect was defined as a region of three (minimum) or more nuclei that had aberrant morphology or a region of similar size that had aberrant actin structures. Defects were scored as either occurring within the region of high injected antibody concentration (correlated) or not (uncorrelated). If defects were detected, they were examined in detail at 1,000×. Any embryos with obvious defects resulting from mechanical damage during sample preparation, injection, or devitellinization, or embryos that were so abnormal that the defects could not be easily assigned to either class were excluded from the scoring. Embryos occasionally had more than one area with defects; these were scored as follows: If an embryo had defects of approximately equal extent in both high antibody and low antibody regions, then it was scored as having an uncorrelated defect. If an embryo had defects in both high antibody and low antibody regions, but one region had a substantially more extensive defect, it was scored as having a defect in the area with more extensive defect. In embryos with more than one defect, it was usually the case that the more extensive defect was in the region of high antibody concentration. It was only rarely the case that defects were more extensive in the region of low antibody concentration. Observations were documented on hypersensitized Technical Pan film (hypersensitization materials from Lumicon, Livermore, CA; film from Eastman Kodak Co., Rochester, NY).

Results

Inhibition of Actin Binding by Anti–95F Myosin Polyclonal Antibody

The effect of affinity-purified anti–95F myosin polyclonal antibody on actin binding in vitro was assessed by immobilizing 95F myosin from *Drosophila* embryo extracts to protein A agarose beads via the anti–95F myosin mAb 3C7, adding anti–95F myosin polyclonal antibody and F-actin, pelleting the beads, and quantifying the pelleted 95F myosin and actin. When no mAb 3C7 was used, no 95F myosin was bound to the beads and only a very small amount of actin pelleted (Fig. 2 *A*). However, when 3C7 was bound to the beads, 95F myosin was also bound and the amount of actin that copelleted with the beads increased substantially (Fig. 2 *A*). When beads containing bound 95F myosin were treated with anti–95F myosin polyclonal antibody, the amount of pelleted actin decreased (Fig. 2 *A*). In four experiments (Fig. 2 *B*), the polyclonal antibody inhibited between 35 and 80% of actin binding (56% average, SD of 19).

Defects in Nuclei Associated with Loss of 95F Myosin Function

We have previously shown that 95F myosin associates with cytoplasmic particles in the embryo cortex and that these particles undergo 95F myosin–mediated transport (Mermall et al., 1994). The particles associate with the actin-based metaphase furrows that form during mitosis. The furrows are required for normal cortical organization. To determine whether 95F myosin plays a role in maintaining the organization of the embryo cortex, its activity was inhibited in living embryos with affinity-purified polyclonal antibody specific for the 95F myosin heavy chain (Kellerman and Miller, 1992; Mermall et al., 1994). This antibody inhibits the association between 95F myosin and F-actin (as previously described) and blocks the particle translocation catalyzed by 95F myosin (Mermall et al., 1994). Anti–95F myosin or control antibodies were microinjected into syncytial blastoderm embryos. The injected embryos were allowed to develop for one to two additional nuclear cycles, fixed, and stained with DAPI to examine nuclear position and morphology. Since the cortical nuclei form a regular, evenly spaced monolayer just beneath the plasma membrane, their arrangement is a highly sensitive indicator of cortical organization. Aberrant nuclear distribution and morphology can result from misorganization of both the actin (Zalokar and Erk, 1976; Postner et al., 1992; Sullivan et al., 1993*b*) and microtubule (Warn et al., 1987; Sullivan et al., 1990) cytoskeletons. Thus, by scoring nuclear defects, we can detect perturbations in either actin or microtubule function. Nuclei that undergo aberrant divisions appear abnormal in shape and size and are sometimes lost from the embryo cortex in subsequent nuclear cycles

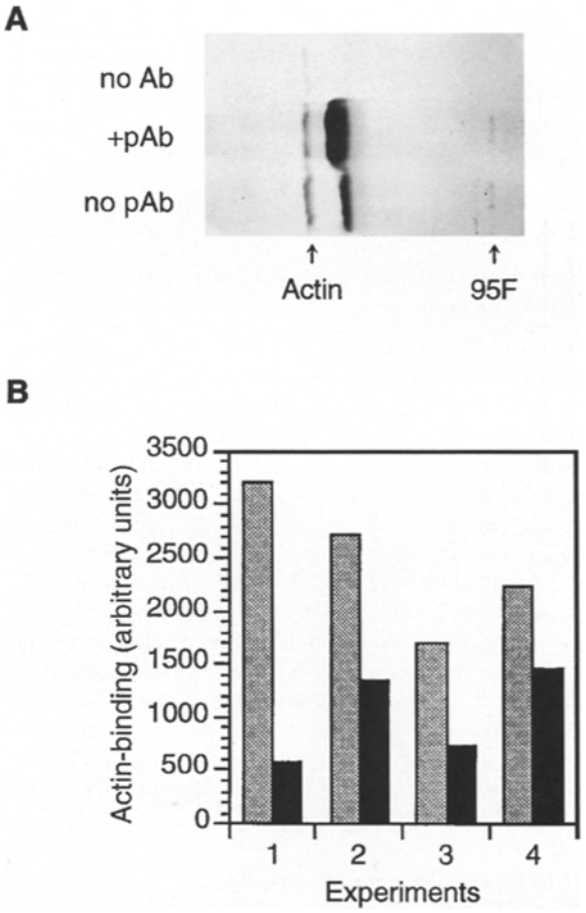

Figure 2. Inhibition of actin binding by anti–95F myosin polyclonal antibody. (*A*) Coomassie blue–stained gel showing proteins that pellet with protein A beads incubated with *Drosophila* embryos extract and actin without bound mAb 3C7 (*no Ab*), with bound mAb 3C7 in the presence of anti–95F myosin polyclonal antibody (*+pAb*), or with bound mAb 3C7 in the absence of anti–95F myosin polyclonal antibody (*no pAb*). Arrows indicate bound 95F myosin (*95F*) and pelleted actin (*Actin*). The darkly stained band in the +pAb lane is the monoclonal and polyclonal antibodies, and that in the no pAb lane is the monoclonal antibody. (*B*) Inhibition of actin binding by anti–95F myosin polyclonal antibody in four separate experiments. The amount of actin pelleted was normalized for the amount of bound 95F myosin. Shaded bars show actin pelleted by protein A beads carrying 95F myosin immobilized by mAb 3C7, and solid bars show actin pelleted by protein A beads carrying 95F myosin immobilized by mAb 3C7 in the presence of anti–95F myosin polyclonal antibody.

(Warn et al., 1987; Minden et al., 1989; Sullivan et al., 1990, 1993*a*; Postner et al., 1992). Since there was limited diffusion of injected antibodies, we identified regions of high antibody concentration using a fluorescent secondary antibody and correlated the position of defects with respect to these regions. Regions of the embryo that contained little injected antibody served as an internal control. We focused on embryos fixed during nuclear cycles 12 and 13, since these embryos had gone through at least one cycle in which metaphase furrows formed under the influence of antibody. Furthermore, a high degree of organization is required to maintain the fidelity of nuclear divisions during these nuclear cycles as neighboring mitotic spindles are in close proximity.

When anti–95F myosin antibodies were injected, many nuclear defects were observed. In regions where antibody concentration was high, some nuclei were elongated or multipolar whereas others were enlarged but round (Fig. 3, *F*, *H*, and *J*), suggesting that the nuclei collided with their neighbors or failed to complete karyokinesis and fused. In some regions nuclei were missing from the cortical cytoplasm (Fig. 3, *F* and *H*). In these regions, nuclei were often visible below the normal apical cortical layer (out of focus nuclei in Fig. 3 *H*). This type of defect is consistent with division failures in previous nuclear cycles (Minden et al., 1989; Sullivan et al., 1990, 1993*a*). Aberrations in nuclear spacing were also seen (Fig. 3, *F* and *H*). In some embryos the number and morphology of the nuclei were normal, and only spacing of the nuclei was abnormal (data not shown). In some embryos small dots of DAPI staining were present, perhaps representing chromosomes lost from nuclei during aberrant divisions (Fig. 3, *F*, *upper portion*). Often, several types of nuclear defects were seen in the same embryo.

Regions of nuclear defects most frequently correlated with the area where the injected anti–95F myosin antibody concentration was high (Fig. 3, compare antibody distribution in *D* with nuclear morphology and distribution in *E*). 47% (n = 145) of antibody-injected embryos had nuclear defects that correlated with the position of high antibody concentration (Fig. 3, *E*, *F*, *H*, and *J*), whereas few defects were found in regions of low anti–95F myosin antibody concentration (Fig. 3, *G*, *I*, and *K*). In embryos injected with control antibodies, few correlated nuclear defects were seen (17% had defects; 72% had normal nuclei; Fig. 3, *A–C*). A small number of embryos had defects (~10%) that did not correlate with the site of high antibody concentration in both control and anti–95F myosin antibody–injected embryos. We speculate that these uncorrelated defects occurred naturally or resulted from the handling of embryos during preparation for injection and fixation.

In addition to the substantial quantitative difference between experimental and control embryos, there were also qualitative differences. In many embryos injected with anti–95F myosin antibody, the defective region was coextensive with the spread of antibody. This was rarely the case when correlated defects were found in control in-

Figure 3. Defects in nuclei associated with anti–95F myosin antibody injection. Injected antibody distribution, visualized with anti-rabbit fluorescent secondary antibody, is shown in *A* and *D*. DAPI staining of DNA is shown in all other panels. The embryo shown in *A–C* was injected with control antibody (anti-GST); all others were injected with anti–95F myosin antibody. (*A*) The injected control antibody has diffused through the middle of the embryo, but the evenly spaced array of nuclei (*B*) is not disturbed. The normal progression through the mitotic stages from the pole (*lower right*) to the center of the embryo can be seen. The arrow indicates the area of high magnification shown in *C*. (*C*) A high magnification view from the region of high injected antibody concentration. Note the normal arrangement and morphology of nuclei. (*D*) Injected anti–95F myosin antibody has diffused through approximately two thirds of the embryo. (*E*) DAPI staining of the embryo shown in *D* reveals a large defect correlated with the region of high antibody concentration. The arrow

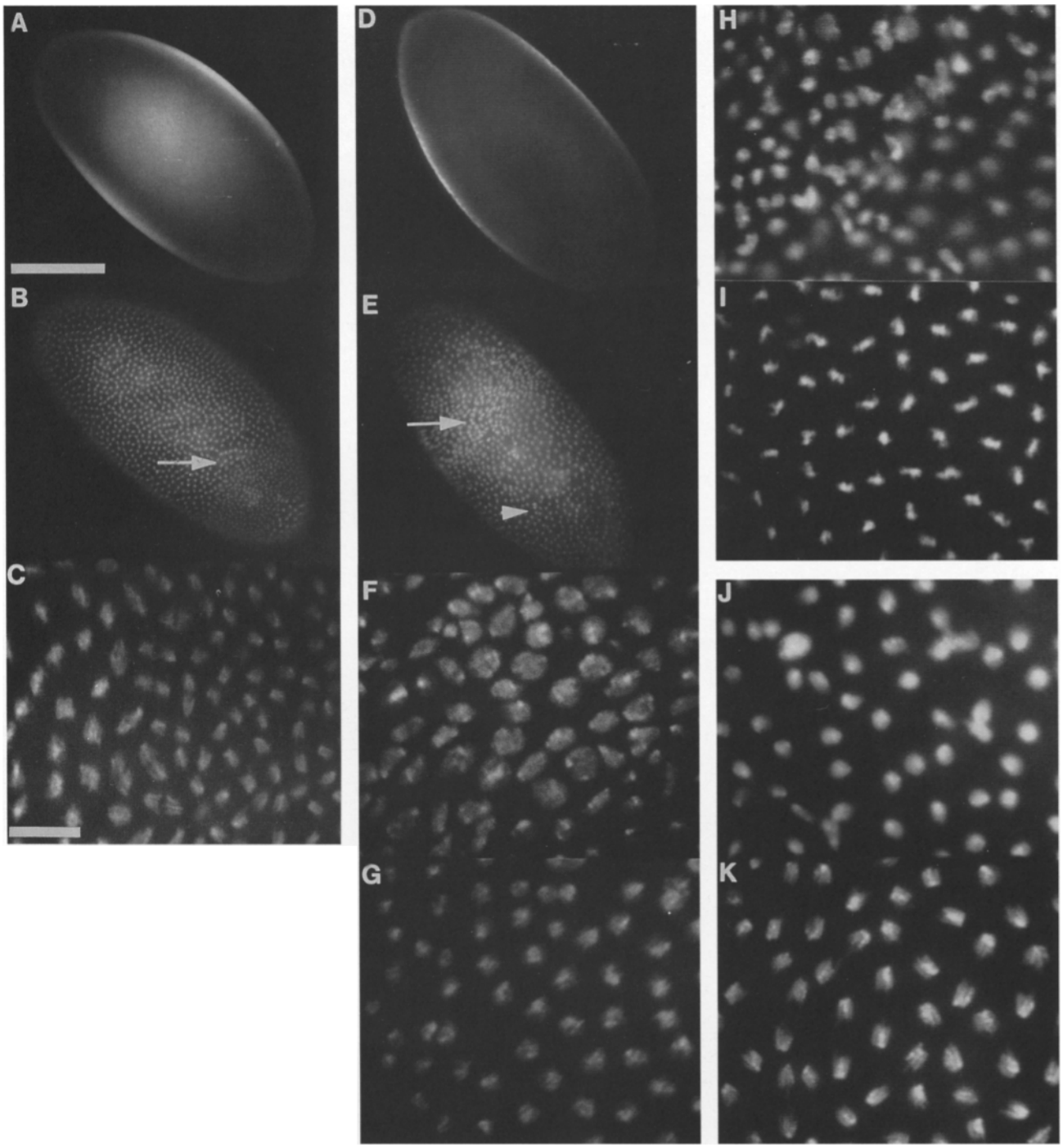

indicates the area of high magnification shown in *F*. The arrowhead marks the region of high magnification shown in *G*. (*F*) High magnification view of nuclear defects in the region of high antibody concentration from the embryo shown in *D*. Large, misshapen, and small nuclei are visible. Nuclear spacing is also aberrant. (*G*) High magnification view of the region of low antibody concentration from the embryo shown in *D*. Note that the region shown is at the edge of the high antibody concentration region. Nuclear spacing, size, and shape are very regular. Although minor defects can be seen (several nuclei are closer together than is normal), the defects are slight when compared with those seen in the region of high antibody concentration. This embryo is an example of one in which defects both correlated and uncorrelated with antibody were present. It was scored as having a correlated defect. (*H* and *I*) Regions of high and low injected antibody concentration, respectively, from another embryo injected with anti–95F myosin antibody are shown at high magnification. In *H* (high antibody concentration), nuclear spacing is abnormal, many of the nuclei are abnormally shaped, and many of the nuclei are out of the plane of focus, indicating that they have moved away from the cortex. Enlarged, small, and fused, multipolar nuclei can also be seen. In *I* (low concentration), nuclear spacing is regular and all of the nuclei are the same size. (*J* and *K*) Similar regions from a different embryo injected with anti–95F myosin antibody are shown. Nuclear defects are seen in the region of high antibody concentration (*J*), whereas no defects are seen in the region of low antibody concentration (*I*). In all examples (*F*, *H*, and *J*), there is a correlation between high antibody concentration and gross nuclear defects. Bars: (*A*) 100 μm; (*C*) 10 μm.

Table I. Percentage of Embryos with Nuclear Defects

	Enlarged	Missing	Spacing	Misshapen	# Scored
Control correlated*	2	17	0	2	99
Control uncorrelated	1	10	1	2	99
Anti-myosin correlated	24	26	6	6	143
Anti-myosin uncorrelated	3	4	1	1	143

*Correlated and uncorrelated indicate whether the listed defect is localized in the region of high injected antibody concentration. Control injections were performed with anti-GST antibodies. Embryos with obvious injection or handling damage were not scored. Some embryos have more than one class of defect.

jected embryos. In these embryos the defective region was frequently localized to a smaller region than the antibody. This qualitative difference was not reflected in the quantitative scoring.

To determine whether the types of nuclear defects occurring from the loss of 95F myosin function were distinct from those that result from nonspecific effects, we examined the types of defects in both control and anti–95F myosin antibody injections. For this analysis, we divided nuclear defects into four different classes: (*1*) enlarged, fused or multipolar nuclei; (*2*) nuclei missing from the apical cortex; (*3*) aberrant spacing; and (*4*) other misshapen but not enlarged nuclei. The class of elongated, fused, bridged, or multipolar nuclei occurred with much greater frequency in anti–95F myosin–injected embryos (24%) than in controls (2%; Table I). These types of nuclear defects have been shown to result from aberrant syncytial divisions (Sullivan et al., 1990, 1993*b*; Postner et al., 1992). The class of missing nuclei occurred with somewhat higher frequency in embryos injected with anti–95F myosin antibodies (26%) than in those injected with control antibodies (17%), but the difference in frequency was not as dramatic. Missing nuclei can result from prior aberrant nuclear divisions (Minden et al., 1989; Sullivan et al., 1990, 1993*a*). However, other forms of damage may also cause this defect, since it was seen at relatively high frequency in the uncorrelated defect class. The other defect classes also occurred with greater frequency when anti–95F myosin antibodies were injected, but the differences in frequency were small when compared with control or uncorrelated defects. This analysis suggests that the class of nuclear defect encompassing enlarged or multipolar nuclei is specific for loss of 95F myosin function.

Defects in Spindles Associated with Loss of 95F Myosin Function

The nuclear defects we observed were consistent with a disruption of the organization of the embryonic cortex allowing inappropriate interactions between nuclei. To de-

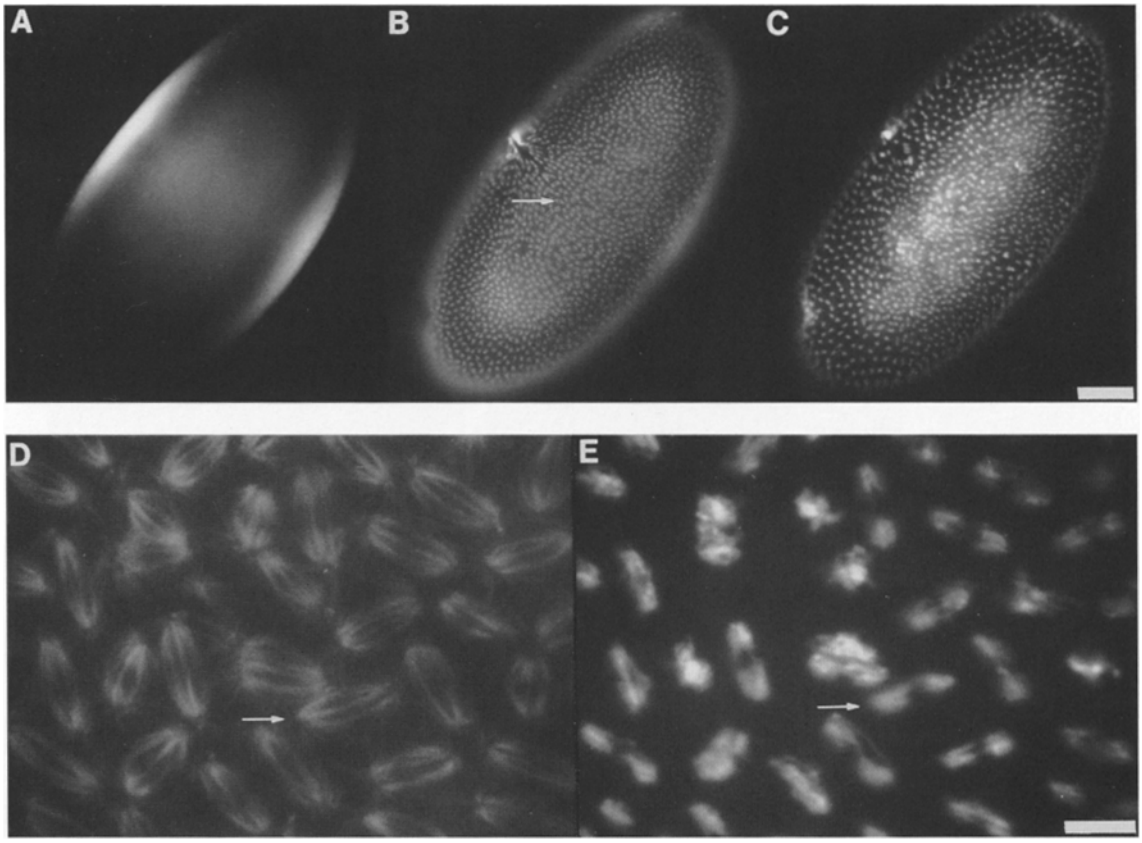

Figure 4. Defects in spindle and nuclear morphology in an embryo injected with anti–95F myosin antibody. (*A*) Localization of injected polyclonal anti–95F myosin antibody visualized with fluorescent secondary antibody. The injection was in the middle of the embryo, and antibodies have diffused throughout the middle region. The injection wound is visible at the top edge of the embryo. (*B*) Anti-tubulin fluorescence. (*C*) DNA staining. Defects in spindle and nuclear morphology and spacing are found in the region of high antibody concentration. (*D*) High magnification view of tubulin staining from the region indicated by the arrow in *B*. Spindles are seen to collide (*arrow*). Some microtubules appear to span from spindle to spindle. (*E*) High magnification view of DNA staining. Some nuclei appear to have fused (see nuclei above *arrow*); other anaphase figures appear poorly defined (*arrow*). Bars: (*C*) 50 μm; (*E*) 5 μm.

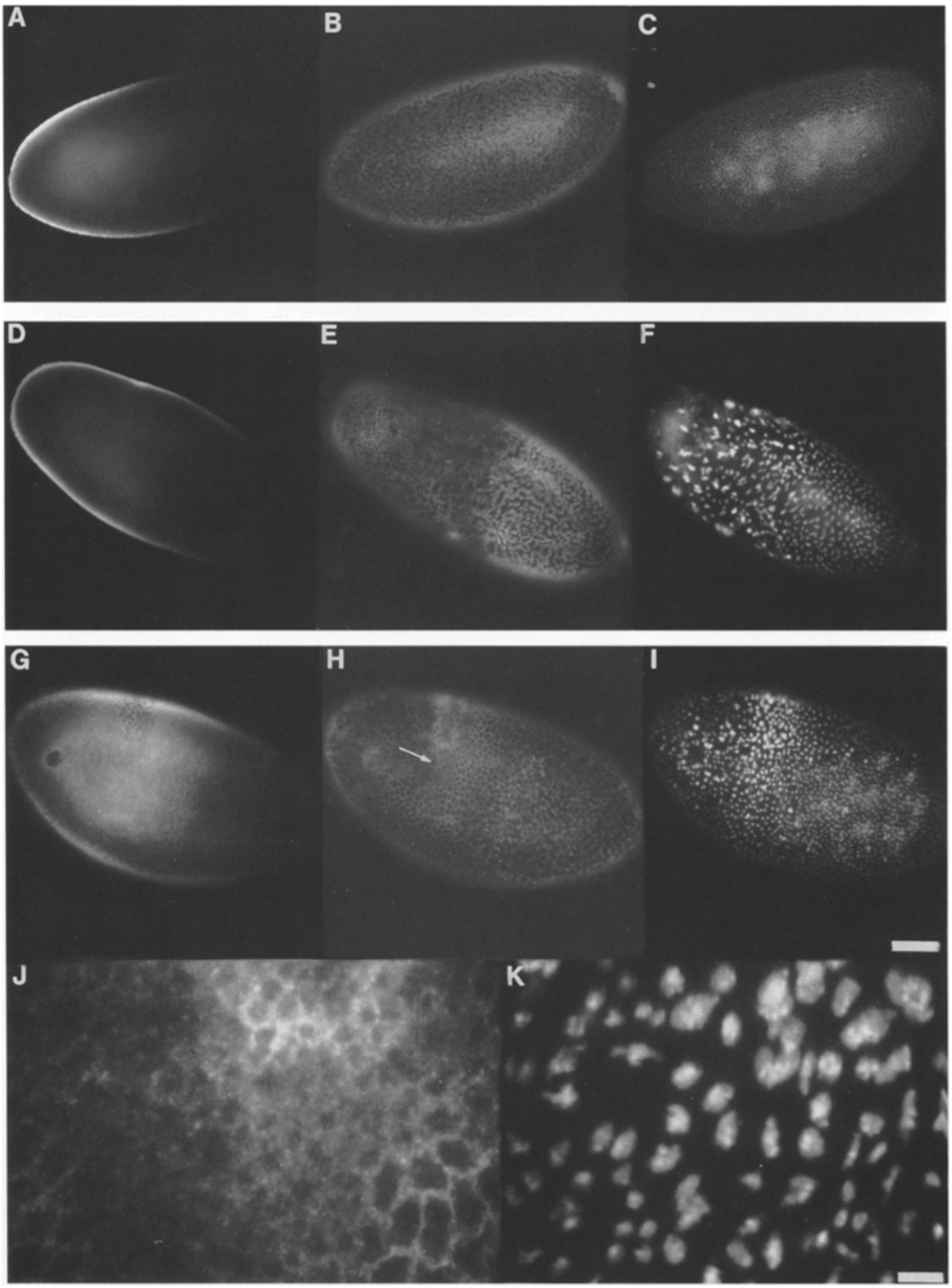

Figure 5. Defects in the actin cytoskeleton and nuclei associated with anti–95F myosin antibody injection. The embryo in the top row was injected with a control antibody (anti-GST), whereas other embryos were injected with anti–95F myosin antibodies. The distribution of injected antibodies is shown in *A*, *D*, and *G*; actin staining is shown in *B*, *E*, *H*, and *J*; DNA staining is shown in *C*, *F*, *I*, and *K*. Embryos injected with control antibodies do not show specific defects (*top row*). Embryos injected with anti–95F myosin antibodies shown disruptions of the pattern of actin staining. Actin defects colocalize with the injected antibodies (compare *D* with *E* and *G* with *H*). The arrow in *H* indicates the region shown at higher magnification in *J* and *K*; note that actin disruptions correlate with enlarged, multipolar nuclei (also compare *E* with *F* and *H* with *I*). Many nuclei appear to be fused or bridged. Bars: (*I*) 50 μm; (*K*) 2.5 μm.

termine whether these nuclear defects were produced by a failure to maintain separation of mitotic spindles, we examined spindles in embryos injected with anti–95F myosin antibodies or control antibodies. Immunofluorescence labeling of tubulin in embryos injected with control (anti-GST) or anti–95F myosin antibodies and localization of the injected antibody demonstrated that defects in the microtubule cytoskeleton correlated with the position of the injected anti–95F myosin antibodies (Fig. 4). In regions of high antibody concentration, we observed colliding mitotic spindles (Fig. 4, *D* and *E*, *arrows*). Microtubules from one spindle also crossed over to neighboring spindles and appeared to interact with those spindles (Fig. 4 *D*); they may also interact with inappropriate chromosomes. These interactions can result in the misassortment of chromosomes and fused, multipolar nuclei (Sullivan et al., 1990). We also observed centrosomes without associated microtubule structures (data not shown), perhaps generated by defective nuclei that had sunk into the interior, leaving their centrosomes behind (Sullivan et al., 1990; Yasuda et al., 1991). In addition, spindles with aberrant morphology were observed, and these aberrant spindles were associated with defects in nuclear morphology (Fig. 4). Some spindles appeared shorter and wider than normal and were associated with multiple nuclei (see top spindle in collision marked with arrows in Fig. 4, *D* and *E*). These dramatically misshapen spindles may have resulted from mitotic aberrations in previous cycles, since defective nuclei were already apparent.

Defects in the Actin Cytoskeleton Are Associated with Loss of 95F Myosin Function

The types of defects seen in microtubule structures and nuclei are consistent with the failure of the actin-based metaphase furrows to form a barrier between adjacent mitoses (Postner et al., 1992; Sullivan et al., 1993*b*). To assess the integrity of the actin cytoskeleton embryos injected with anti–95F myosin antibody were stained with fluorescently labeled phalloidin to visualize F-actin. In regions of high antibody concentration, we found defects in the actin cytoskeleton (Fig. 5, *D* and *E*, *G* and *H*, and *J*). There was a dramatic correlation between regions with disrupted actin and regions of high antibody concentration (Fig. 5, compare *D* with *E* and *G* with *H*). Some actin furrows and caps were fuzzy or indistinct. In fuzzy furrows, the lines of actin staining were broad and less crisply defined than normal (Fig. 5, *H* and *J*). We also observed regions of reduced or diffuse actin staining (Fig. 5, upper region of disrupted area of *E*). In some cases, we observed regions where the actin-based furrow spacing was aberrant (Fig. 5, *H* and upper portion of *J*) or regions where caps were smaller than normal. Multiple types of actin defects were found within single embryos. Defects in the actin cytoskeleton were associated with nuclear defects (Fig. 5, *E* and *F*, *H* and *I*, and *J* and *K*) of the types previously described.

Embryos injected with antibodies against 95F myosin had a much greater incidence of actin defects (48% correlated defects, 44% normal; $n = 145$) than embryos injected with control antibodies (16% correlated defects, 77% normal; $n = 105$). A small number of defects (~8%) did not correlate with the site of high antibody concentration in both control and anti–95F myosin antibody–injected embryos. As is the case with nuclear defects, these uncorrelated defects probably resulted from the handling of embryos during preparation for injection and fixation, as well as naturally occurring defects.

To determine whether the types of defects resulting from the loss of 95F myosin were distinct from those resulting from nonspecific effects, we examined the incidence of different types of defects occurring in both anti–95F myosin and control antibody injections. For this analysis, we scored actin defects in five classes: (*1*) fuzzy or indistinct actin structures; (*2*) missing actin structures; (*3*) aberrant spacing of actin caps; (*4*) small mesh actin furrows or small caps; and (*5*) other. A much greater incidence of fuzzy or indistinct actin structures occurred when anti–95F myosin antibodies (25%) were injected than when control antibodies were used (3%; Table II). Actin structures were missing in 25% of embryos injected with anti–95F myosin antibodies, whereas only 10% of the control injected embryos displayed this defect (Table II). Since many more experimental embryos had this defect that controls, the loss of actin structures may have been a direct result of the inhibition of 95F myosin function. However, actin loss could result from the loss of centrosomes (along with their associated nuclei) owing to aberrant divisions in previous nuclear cycles, since centrosomes are involved in the organization of cortical actin structures (Raff and Glover, 1989; Yasuda et al., 1991). In addition, nonspecific damage might have resulted in the loss of actin structure, since this type of defect occurred with relatively high frequency uncorrelated to injected antibody (Table II). Although the other classes of defects occurred with slightly higher frequency in anti–95F myosin–injected embryos than in control injected embryos, the increase in frequency was not very dramatic. These data suggest that fuzzy or indistinct actin structures are specific to the loss of 95F myosin function.

Defects in Actin Structures Correlate with Defects in Nuclear Morphology

The class of nuclei that are elongated, fused, bridged, or multipolar and the fuzzy indistinct actin structures were both specific for the loss of 95F myosin function. We therefore examined whether these two types of defects occurred together, suggesting that the nuclear defects were caused by the actin defect. The elongated, fused, bridged, or multipolar nuclear defects strongly correlated with actin defects (44 of 46 embryos). Most commonly missing (25 of 46 embryos) and/or fuzzy, indistinct (18 of 46 embryos) actin defects were present in regions of nuclear defect (Ta-

Table II. Percentage of Embryos with Actin Defects

	Fuzzy	Missing	Spacing	Small	Other	# Scored
Control correlated*	3	10	2	2	1	99
Control uncorrelated	0	6	0	1	0	99
Anti-myosin correlated	25	25	4	7	4	143
Anti-myosin uncorrelated	1	6	2	0	0	143

*Correlated and uncorrelated refer to the correlatin of the listed defect with the region of high injected antibody concentration. Control injections were performed with anti-GST antibodies. Embryos with obvious injection or handling damage were not scored. Some embryos have more than one class of defect.

Table III. Incidence of Actin Defects Associated with Enlarged, Fused Nuclei

	Missing	Fuzzy	Small	Spacing	Other
Correlated*	25	18	5	4	5
Uncorrelated	4	1	0	1	0

The number of occurrences of different types of actin defects are shown; some embryos have multiple types of defects. 46 embryos injected with anti–95F myosin antibodies with enlarged, bridged, or fused nuclei were scored.
*40 embryos had defects that correlated with the region of high antibody concentration (*Correlated*), 4 embryos had defects that did not correlate to the region of high antibody concentration (*Uncorrelated*), and 2 embryos had nuclear defects but apparently normal actin staining.

ble III and Fig. 5). Since metaphase furrows cannot form when F-actin is missing, it is reasonable that nuclear defects would be present in these regions. However, in many cases actin was present in the correct location, but was not organized properly (Table III). This suggests that actin alone is not sufficient to maintain separation between adjacent mitoses and that 95F myosin and/or the 95F myosin–associated particles are important for proper organization of the actin cytoskeleton.

Defects in Actin Structures Precede Defects in Microtubules

The organizations of the actin- and microtubule-based cytoskeletons of the syncytial blastoderm are interdependent. Centrosomes provide spatial cues for the localization of actin caps and metaphase furrows (Raff and Glover, 1989; Yasuda et al., 1991). In particular, the furrows form between centrosomes of adjacent nuclei. If centrosomes are not properly positioned, furrows normally adjacent to those nuclei may not form (Sullivan et al., 1990). Conversely, if no metaphase furrows form, neighboring spindles interact, leading to microtubule defects (Postner et al., 1992; Sullivan et al., 1993*b*). As a result, actin defects could be the result of defects in the microtubule-based cytoskeleton, or the converse may be true. To determine whether the primary effect of the loss of 95F myosin function is a disruption of the actin cytoskeleton, we examined actin structures in mitotic embryos before gross abnormalities in microtubules and nuclei were evident. In these embryos most spindles had normal morphology and position; therefore we expected normal metaphase furrows. However, this was not the case. One example is shown in Fig. 6. When examined at low power (not shown), this embryo was not grossly abnormal—only minor nuclear and microtubular aberrations were apparent. When examined at high power, most of the actin array (*green*) appeared essentially normal when viewed en face (Fig. 6 *A*). The actin-based metaphase furrows invaginate perpendicular to the embryo surface; thus, actin has a polygonal appearance in an XY view (*A*). Each spindle (*red*) was surrounded by discrete lines of actin staining. To examine furrow structure in detail, we used computational optical sectioning microscopy to obtain three-dimensional images (XZ sections; Fig. 6, *B*, *C*, and *D*). Some furrows and spindles appeared normal, with actin staining extending into the embryo to the depth of the spindles and tubulin staining contained within the domain established by the furrow (Fig. 6, *A*, *C*, and *D*, *brackets*). The actin and tubulin staining in these regions was similar to the distributions of actin

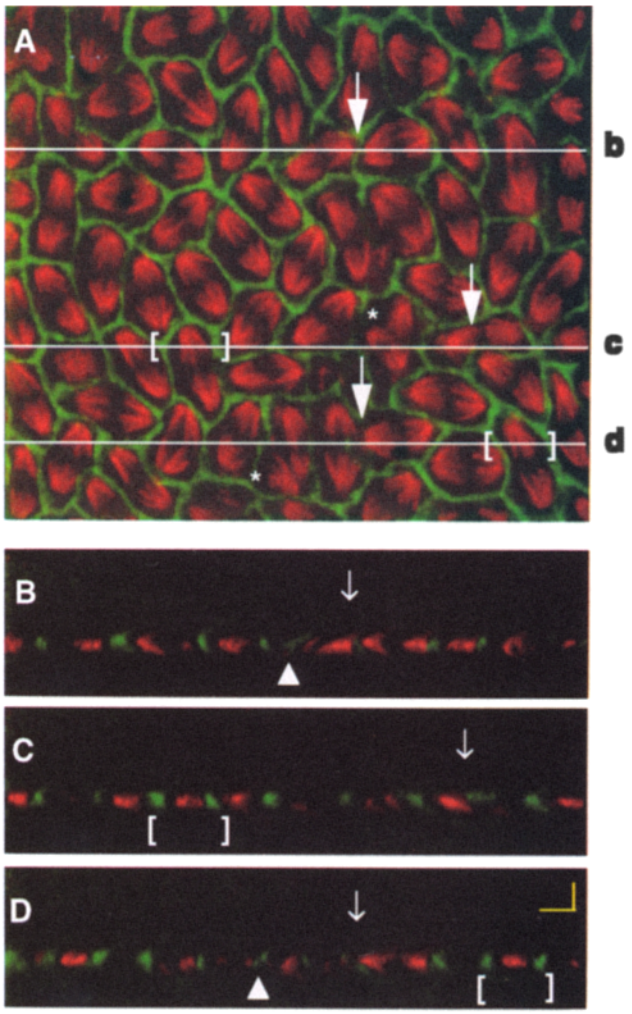

Figure 6. Computational optical sectioning micrographs of an embryo injected with anti–95F myosin antibodies and stained for actin (*green*) and tubulin (*red*). (*A*) XY view of a projection through 32 μm of cortex. Arrows indicate some examples of furrows with gaps or that have a fuzzy, abnormal appearance. Spindles can be seen crossing over or encroaching on these aberrant furrows. Aberrant spindles are marked with asterisks. (*B–D*) XZ slices with the embryo interior toward the bottom of the panels. Lines and lowercase letter (*b–d*) in *A* show the positions of XZ slices shown *B–D*. Some examples of microtubules crossing over defective furrows and furrows that are not invaginated to the proper depth are indicated by arrows, and fuzzy, misorganized furrows are marked with arrowheads. Normal metaphase furrows in which actin invaginates to the depth of the spindles are indicated for comparison (*brackets*). Bar, 5 μm.

and tubulin seen in control injected embryos (not shown) and previously reported (Karr and Alberts, 1986; Sullivan et al., 1993*b*).

In contrast, other regions of the embryo appeared to have slight defects in the actin-based furrows. There were gaps in some furrows and some appeared indistinct (Fig. 6 *A*, *arrows*). These abnormal actin furrows did not seem to function as barriers between spindles; microtubules could sometimes be seen crossing over these actin structures and adjacent spindles could be seen encroaching on neighboring cytoplasmic domains (Fig. 6 *A*, *arrows*). When examined in XZ sections (Fig. 6, *B–D*), some invaginations did

not extend into the embryo to the depth of the spindles (Fig. 6, *C* and *D*, *arrows*). Some furrows appeared fuzzy and misorganized (Fig. 6 *B* and *D*, *arrowheads*). A few aberrant spindles could be seen (Fig. 6 *A*, *asterisks*), but even these aberrant microtubule structures were surrounded by actin in a furrowlike distribution. It is unlikely that the defective actin furrows observed in this embryo resulted from prior microtubule defects, since most spindles appeared normal. However, the encroachment of microtubules from one spindle into neighboring domains that occurred as a result of aberrant actin furrows was likely to be the event that gave rise, after subsequent division cycles, to the gross nuclear defects previously presented (Figs. 3, 4, and 5).

The integrity of the metaphase furrows was further explored by examining the distribution of membrane (stained with Con A), actin, and DNA. Computational optical sectioning microscopy of embryos injected with anti–95F myosin was used to examine these components in three dimensions (Fig. 7). In regions that appeared normal (Fig. 7, *A* and *C*, *brackets*), actin (*red*) and Con A (*green*) were both concentrated in the furrow region (*yellow*). Actin could be seen underlying membrane in invaginations that extended to the depth of the nuclei. Nuclei were found in the cortex, were regularly shaped, and were separated by actin staining. However, in some regions actin and membrane were found in structures that did not extend into the embryo to the normal depth of cortical nuclei (Fig. 7, *arrows*; compare with normal region marked with brackets in *A* and *C*). Nuclei associated with these defective structures were sinking into the embryo's interior. This loss of cortical nuclei was one of the gross defects likely to result from the more subtle defect in metaphase furrow organization (Fig. 6). In both normal and abnormal appearing furrows, actin was frequently found deeper in the embryo than the Con A membrane marker (Fig. 7, *B–C*).

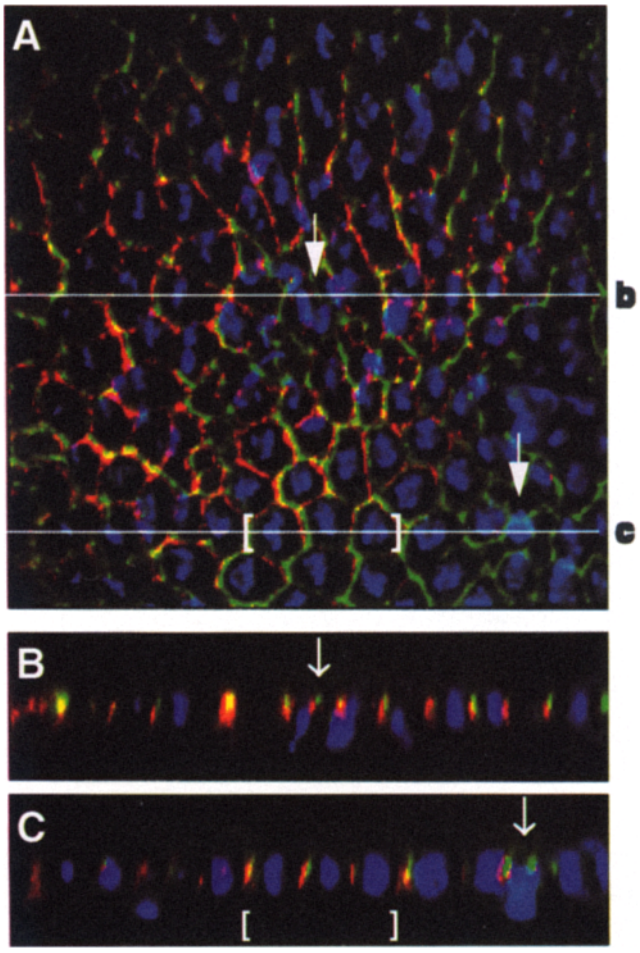

Figure 7. Computational optical sectioning micrographs of an embryo injected with anti–95F myosin antibodies and stained for actin (*red*), membrane (*green*), and DNA (*blue*). (*A*) XY view of a projection through 20 μm of cortex. (*B* and *C*) XZ slices with the embryo interior toward the bottom of the panels. Lines and lowercase letters (*b* and *c*) in *A* show the position of XZ slices shown in *B* and *C*. Actin and membrane partially coincide in a furrowlike distribution, creating the yellow color, but membrane does not invaginate as deeply as actin (XZ views, *B* and *C*). Shallow actin and membrane structures are seen in XZ views and are associated with nuclei sinking into the interior of the embryo (*arrows*, *B* and *C*). One region of normal appearing actin-based metaphase furrows and nuclei is indicated (*brackets*) for comparison. Magnification is the same as in Fig. 6.

Localizatin of 95F Myosin and Actin During Cell Cycle–dependent Redistributions

The nuclear and microtubule defects found were consistent with a failure of metaphase furrows to separate adjacent mitoses. That actin-mediated events underlie these defects was supported by the observed abnormalities in furrow structure. To understand the generation of defects further, we examined the spatial and temporal relationship between 95F myosin and actin during their cell cycle–dependent redistributions. We used fluorescent labeling of fixed embryos to visualize 95F myosin and actin simultaneously. We correlated the distributions of these proteins to the stage of embryonic development and position in the cell cycle by using DAPI to visualize DNA.

During interphase of nuclear cycles 11–13, 95F myosin–associated particles were found throughout the cytoplasmic domains surrounding each nucleus (Fig. 8 *I*). These domains encompass the region in which both actin caps and microtubules associate with each nucleus. Although 95F myosin–associated particles were concentrated in these cytoplasmic domains, they were also found in regions between domains; thus the domain boundaries were not always as clearly defined as those of actin caps. Occasionally, linear elements of 95F myosin fluorescence could be seen extending along the edge of a cytoplasmic domain. F-actin was not found in these linear structures. In early prophase, before the actin has substantially rearranged, 95F myosin accumulated in the region where actin-based metaphase furrows would form (Fig. 8 *P*). Later in prophase, F-actin began to form the polygonal array characteristic of metaphase furrows, and 95F myosin fluorescence coincides with F-actin. This polygonal distribution of actin and 95F myosin remained visible throughout metaphase (Fig. 8 *M*). However, the concentration of 95F myosin in these structures decreased as mitosis proceeded. During anaphase, the mitotic invaginations vanished, and both actin and 95F myosin lost the furrow-like appear-

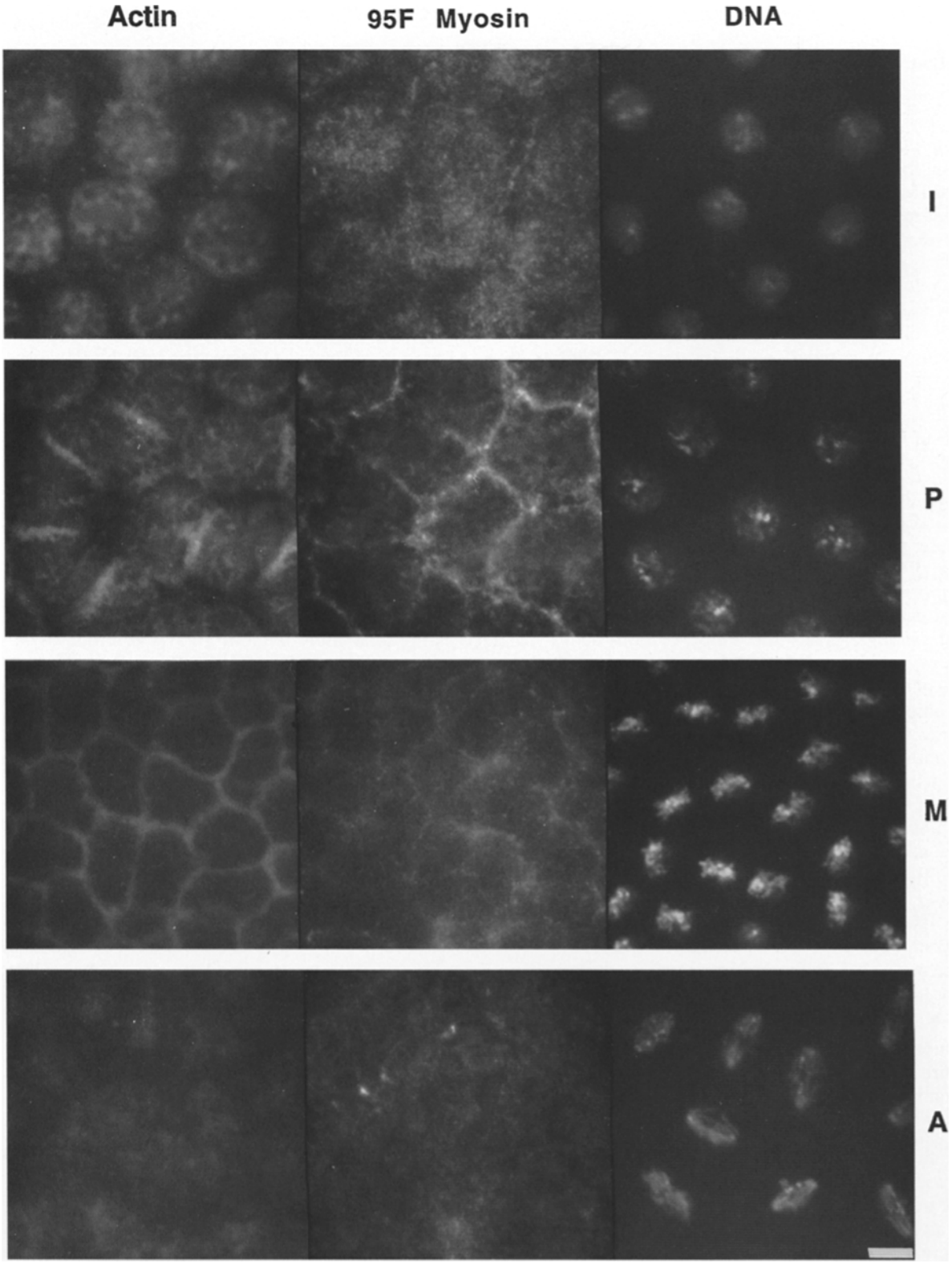

Figure 8. The distribution of 95F myosin in relation to F-actin and DNA. Embryos were stained with fluorescent phalloidin to visualize F-actin (*Actin*), mAb 3C7 and fluorescent secondary antibody to localize 95F myosin (*95F Myosin*), and DAPI (*DNA*). Progression through interphase (*I*), prophase (*P*), metaphase (*M*), and anaphase (*A*) is shown. Bar, 5 μm.

ance; much less organization was evident as actin and 95F myosin returned to their interphase distributions (Fig. 8 *A*). These studies show that 95F myosin enters the region where actin-based furrows will form before most of the actin and also leaves, before actin. 95F myosin is in the right place at the right time to contribute to the formation of normal metaphase furrows, consistent with the defects observed when 95F myosin function was inhibited.

Discussion

Loss of 95F Myosin Function

The studies presented here suggest that the 95F unconventional myosin plays an important role in the early development of *Drosophila* embryos. We have previously shown that this myosin catalyzes transport of cytoplasmic particles in embryos (Mermall et al., 1994). We now show that inhibition of this myosin's function has dramatic effects on embryonic development. Syncytial blastoderm divisions are aberrant, leading to disorganization of the blastoderm. Nuclear morphology and position are affected. The defects we report are similar to defects seen when the actin cytoskeleton is disrupted by drugs (Zalokar and Erk, 1976) or by genetic manipulation (Sullivan et al., 1990, 1993*b*; Postner et al., 1992). Cytochalasin treatment leads to gross abnormalities, including anaphase nuclear collisions, polyploid nuclei, and multiple spindles (Zalokar and Erk, 1976). Embryos derived from females homozygous for the *scrambled* (*sced*) and *nuclear-fallout* (*nuf*) mutations have nuclei that vary in size and shape, abnormal nuclear spacing, and regions devoid of nuclei (Sullivan et al., 1993*b*). In these mutant embryos nuclear defects arise from disruption of the actin-based metaphase furrows that separate neighboring nuclear domains. This leads to spindle defects that cause the aberrant nuclear divisions. Another mutation, *sponge*, causes disruption of both actin caps and furrows; similar nuclear defects are observed (Postner et al., 1992).

The defects observed when 95F myosin function is inhibited are similar to those seen when the actin cytoskeleton is disrupted; therefore, it seems likely that they result from effects on the actin cytoskeleton. We further investigated the generation of these defects by examining the distribution of microtubules and actin in antibody-injected embryos. Our results show that there is a correlation between disruption of 95F myosin function, abnormal actin, abnormal spindles, and defects in nuclear morphology and position. Embryos fixed during mitosis and stained to reveal these cellular components provide evidence of how the defects we see are generated. In the abnormal regions during mitosis, neither actin nor membrane extends into the embryo to the same extent as seen in normal furrows. Actin in the furrowlike structures that are present appears to be poorly organized. Microtubules can be seen crossing over the abnormal furrows, allowing neighboring spindles to interact. During anaphase, spindles often collide, generating large and misshapen nuclei. These data suggest that 95F myosin and/or the particles it transports are required for normal actin-based metaphase furrows to form (Fig. 9).

In this study we found overall rates of embryos with defects (actin and/or nuclear) caused by injection to be 47% (n = 148) for embryos injected with anti–95F myosin antibodies and 18% (n = 107) for control injections. This almost threefold higher rate of defects in experimental versus control embryos indicates that disruption of 95F myosin function, even in only a portion of the embryo, has significant detrimental effects on development. However, defects that did not correlate with injection were also seen. Approximately 10% of both control and experimental embryos have uncorrelated defects. These defects are most likely to be nonspecific and are equally likely to occur in any region of the embryo. Therefore, nonspecific defects that occur in regions of high antibody concentration would be scored as correlated defects. If the estimated number of nonspecific defects scored as correlated are subtracted out as background, the percentage of embryos with correlated defects is approximately fivefold greater in embryos injected with anti–95F myosin antibody than in controls.

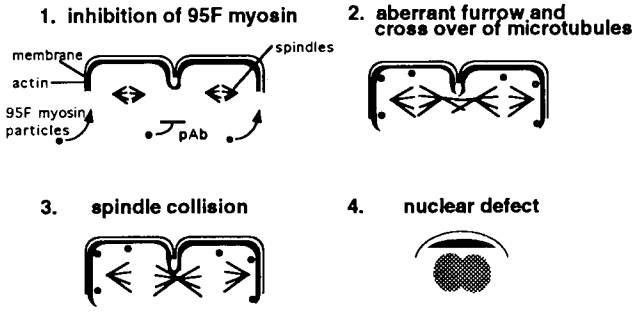

Figure 9. Model for the generation of defects due to loss of 95F myosin function. (*1.*) Transport of 95F myosin–associated particles is blocked by antibody. (*2.*) Actin-based furrows do not form correctly without the contribution of 95F myosin–associated particles. As a result, microtubules from one nuclear domain can interact with neighboring domains. (*3.*) Inappropriate microtubule interactions lead to spindle collisions across defective actin-based furrows. (*4.*) Spindle collisions result in the fusion of adjacent nuclei.

Although there is a substantial difference in the rates of defects seen in experimental versus control embryos, it is likely that we underreport the number of embryos affected by anti–95F myosin antibody. This may be due to several factors. These defects were initially detected in low power scans of slides. In most cases, only one side of an embryo could be examined; if a defect was present on the other side of an embryo (away from the lens), that embryo may have been scored as normal. It is also likely that nascent defects were missed in some experiments, as such defects may not have been visible at low power. For example, the actin furrows in Fig. 6 would not have been scored as defective since they appear relatively normal when viewed en face. A three-dimensional examination of these furrows was required to see their defects. In addition to difficulties in detecting defects, antibody injection may not produce defects in every injected embryo. The location, timing, and quantity of injected antibody may play a role in the generation of defects. More importantly, not every disruption of actin-based metaphase furrows will produce dramatic defects in other cellular components. In *sponge* embryos there is a total loss of metaphase furrows, but substantial numbers of aberrant spindles and nuclei are not seen until mitosis of cycle 12 (Postner et al., 1992). This implies that embryos lacking 95F myosin function during the mitosis of cycle 11 and fixed in cycle 12 should not be expected to have substantial nuclear defects, even if furrows are widely disrupted.

Our previous studies showed that the anti–95F myosin antibody blocks the transport of 95F myosin–associated particles in vivo (Mermall et al., 1994). This previous study used a lower concentration of antibody. Transport was affected only in a small area for a limited time period. In the

current study, higher antibody concentrations were used to disrupt 95F myosin function over a region large enough to produce scorable defects. At the antibody concentration used in this study, 95F myosin may precipitate within the cell (data not shown). It is unlikely that precipitated 95F myosin can mediate transport. However, in some cases anti–95F myosin antibody appears in a furrowlike distribution after the embryo has completed mitosis (data not shown). If 95F myosin was in furrows when the antibody was injected, it may remain in a furrlowlike distribution owing to precipitation or loss of transport function. However, we do not know whether this antibody distribution reflects endogenous 95F myosin protein distribution. The large amount of anti–95F myosin antibody already present makes it difficult to determine the distribution of 95F myosin in antibody-injected embryos.

Localization of 95F Myosin

The localization of 95F myosin in relation to F-actin supports the conclusion that 95F myosin is required for normal actin-based structures. 95F myosin–associated particles are found in cytoplasmic domains around the nuclei during interphase. Early in mitosis, 95F myosin is concentrated in the region where the actin-based metaphase invaginations will form. We have observed the 95F myosin–dependent translocation of 95F myosin–associated particles to the metaphase furrow region (Mermall et al., 1994). The redistribution of 95F myosin occurs while most F-actin is still in interphase caps, although some F-actin must be present in the intercap region to support the 95F myosin–dependent translocation of particles. As mitosis proceeds and actin-based metaphase furrows are evident, 95F myosin becomes less concentrated in these structures. These data suggest that, in response to cell cycle cues, 95F myosin undergoes a redistribution to the metaphase furrow region before the redistribution of most of the F-actin. Thus, 95F myosin is in the proper location at the proper time to participate in the formation of the metaphase furrows. F-actin in the early embryo colocalizes at particular times with a large number of actin-binding proteins; including 95F myosin (Miller et al., 1989). As these proteins mediate the formation and dynamics of actin structures (Weeds, 1982; Pollard and Cooper, 1986), it is reasonable that 95F myosin and/or the 95F myosin–associated particles may contribute to the formation of these actin-based structures.

The redistribution of 95F myosin in response to cell cycle cues may be accomplished through mechanisms similar to those used to regulate the activity of other unconventional myosins. Some *Acanthamoeba* and *Dictyostelium* myosin I molecules require phosphorylation of a conserved serine or threonine residue in the head domain for maximal ATPase activity (Tan et al., 1992). Both 95F myosin and porcine myosin VI, a 95F myosin homologue, contain a threonine at this conserved site (Hasson and Mooseker, 1994). Association with light chains provides another regulatory route. The actin-activated ATPase and motile activity of several unconventional myosins are regulated by calmodulin light chains in vitro (Collins et al., 1990; Cheney et al., 1993*a*; Wolenski et al., 1993). Both *Drosophila* and porcine myosin VI possess a putative calmodulin-binding IQ domain (Kellerman and Miller, 1992; Hasson and Mooseker, 1994), and porcine myosin VI has been shown to bind calmodulin (Hasson and Mooseker, 1994). Porcine myosin VI distribution appears to be regulated by a developmental signal (Hasson and Mooseker, 1994). Like 95F myosin's cell cycle redistribution, regulation of its distribution in response to specific signals may also be important for its function. Porcine myosin VI is associated with the apical brush border in kidney proximal tubule, where it is hypothesized to play a role in membrane recycling (Hasson and Mooseker, 1994). 95F myosin's role in transport would lend support to this speculation. However, it remains to be demonstrated whether porcine myosin VI is involved in transport of cytoplasmic components, as is 95F myosin.

Potential Functions of 95F Myosin

What role may 95F myosin and/or its associated particles play in metaphase furrow function? The presence of actin at the sites where metaphase furrows would normally form in embryos injected with anti–95F myosin antibody suggests that 95F myosin is not required to recruit actin to the furrow region. Although actin is often present, normal invaginations do not form.

Since other unconventional myosins interact with both membrane and F-actin, an attractive hypothesis is that 95F myosin forms a structural link between F-actin in the furrows and the plasma membrane. However, if 95F myosin does play a role in linking actin to the membrane, it is unlikely that 95F myosin is the only link, as it leaves the furrows before actin. An alternative idea is that 95F myosin provides the force required for actin invagination. This idea is supported by the observation of shallow membrane and actin in abnormal furrows seen in embryos injected with anti–95F myosin antibody. However, cytoplasmic myosin, a force-generating molecule that is associated with cleavage furrows, is also present in metaphase furrows (Young et al., 1991). It seems likely that this conventional myosin may play a role in force generation here as well. Thus, we do not favor the hypothesis that 95F myosin is generating force. Instead, we suggest that 95F myosin may be indirectly involved in furrow formation through the delivery of required components (Fig. 9). The particles 95F myosin transports to the furrows may contribute proteins and/or lipids that are important for furrow formation, organization, or structural integrity. The absence of these materials would cause the misorganization of actin and the lack of normal invaginations that we observe.

Conclusion

In this study we have shown that the 95F unconventional myosin plays an important role in generating normal actin-based structures in the *Drosophila* embryo. This is one of the few unconventional myosins for which a specific function has been demonstrated.

We would like to thank Drs. John Cooper and Jim McNally for consistent support throughout the course of this work. We thank Keith Doolittle for assistance with image processing and the Biomedical Computing Laboratory for computer support. We are grateful for the encouragement and advice we received from members of the Miller lab throughout the course of this work and for their careful reading of the manuscript. We are espe-

cially grateful to Dr. Ginger Armbrust for her critical reading of the manuscript and advice on data presentation.

This work was accomplished using the Department of Biology optical sectioning microscope, which was purchased with funds from National Institutes of Health (NIH) equipment grant 1 S10 RR 047 5501. This work was supported by NIH grant GM-43607 to K. G. Miller.

Received for publication 21 November 1994 and in revised form 3 March 1995.

References

Adams, R. T., and T. D. Pollard. 1986. Propulsion of organelles isolated from *Acanthamoeba* along actin filaments by myosin I. *Nature (Lond.)*. 322:754–756.

Agard, D. A., Y. Hiraoka, P. Shaw, and J. W. Sedat. 1989. Fluorescence microscopy in three dimensions. *Methods Cell Biol.* 30:353–377.

Ashburner, M. 1989. *Drosophila*: A Laboratory Manual. Cold Spring Harbor Laboratory Press, Cold Spring Harbor, NY.

Baines, I. C., H. Brzeska, and E. D. Korn. 1992. Differential localization of *Acanthamoeba* myosin I isoforms. *J. Cell Biol.* 119:1193–1203.

Bement, W. M., and M. S. Mooseker. 1993. Molecular motors: keeping out the rain. *Nature (Lond.)*. 365:785–786.

Bement, W. M., T. Hasson, J. A. Wirth, R. E. Cheney, and M. S. Mooseker. 1994. Identification and overlapping expression of multiple unconventional myosin genes in vertebrate cell types. *Proc. Natl. Acad. Sci. USA*. 91:6549–6553.

Cheney, R. E., and M. S. Mooseker. 1992. Unconventional myosins. *Curr. Opin. Cell Biol.* 4:27–35.

Cheney, R. E., M. K. O'Shea, J. E. Heuser, M. V. Coelho, J. S. Wolenski, E. M. Espreafico, P. Forscher, R. E. Larson, and M. S. Mooseker. 1993*a*. Brain myosin-V is a two-headed unconventional myosin with motor activity. *Cell*. 75: 13–23.

Cheney, R. E., M. A. Riley, and M. S. Mooseker. 1993*b*. Phylogenetic analysis of the myosin superfamily. *Cell Motil. Cytoskel.* 24:215–223.

Collins, K., J. R. Sellers, and P. Matsudaira. 1990. Calmodulin dissociation regulated brush border myosin I (110-kD-calmodulin) mechanochemical activity in vitro. *J. Cell Biol.* 110:1137–1147.

DeLozanne, A., and J. Spudich. 1987. Disruption of the *Dictyostelium* myosin heavy chain gene by homologous recombination. *Science (Wash. DC)*. 236: 1086–1091.

Doberstein, S. K., I. C. Baines, G. Wiegand, E. D. Korn, and T. D. Pollard. 1993. Inhibition of contractile vacuole function *in vivo* by antibodies against myosin-I. *Nature (Lond.)*. 365:841–843.

Fath, K. R., and D. R. Burgess. 1993. Golgi-derived vesicles from developing epithelial cells bind actin filaments and possess myosin-I as a cytoplasmically oriented peripheral membrane protein. *J. Cell Biol.* 120:117–127.

Fath, K. R., G. M. Trimbur, and D. R. Burgess. 1994. Molecular motors are differentially distributed on Golgi membrans from polarized epithelial cells. *J. Cell Biol.* 126:661–675.

Foe, V. E., and B. M. Alberts. 1983. Studies of nuclear and cytoplasmic behavior during the five mitotic cycles that precede gastrulation in *Drosophila* embryogenesis. *J. Cell Sci.* 61:31–71.

Fukui, Y., T. J. Lynch, H. Brzeska, and E. D. Korn. 1989. Myosin I is located at the leading edges of locomoting *Dictyostelium* amoebae. *Nature (Lond.)*. 341:328–331.

Hafen, E., A. Kuroiwa, and W. J. Gehring. 1984. Spatial distribution of transcripts from the segmentation gene *fushi tarazu* during *Drosophila* embryonic development. *Cell*. 37:833–841.

Hasson, T., and M. S. Mooseker. 1994. Porcine myosin-VI: characterization of a new mammalian unconventional myosin. *J. Cell Biol.* 127:425–440.

Huxley, H. E. 1969. The mechanism of muscular contraction. *Science (Wash. DC)*. 164:1356–1366.

Joshi, S., and M. I. Miller. 1993. Maximum *a posteriori* estimation with good's roughness for three-dimensional optical-sectioning microscopy. *J. Opt. Soc. Am.* 10:1078–1085.

Karess, R. E., X.-J. Chang, K. A. Edwards, S. Kulkarni, I. Aguilera, and D. P. Kiehart. 1991. The regulatory light chain of nonmuscle myosin is encoded by *Spaghetti-Squash*, a gene required for cytokinesis in Drosophila. *Cell*. 65: 1177–1189.

Karr, T. L., and B. M. Alberts. 1986. Organization of the cytoskeleton in early *Drosophila* embryos. *J. Cell Biol.* 102:1494–1509.

Kellerman, K. A., and K. G. Miller. 1992. An unconventional myosin heavy chain gene from *Drosophila melanogaster*. *J. Cell Biol.* 119:823–834.

Kellogg, D. R., T. J. Mitchison, and B. M. Alberts. 1988. Behavior of microtubules and actin filaments in living *Drosophila* embryos. *Development*. 103: 675–686.

Knecht, D. A., and W. F. Loomis. 1987. Antisense RNA inactivation of myosin heavy chain gene expression in *Dictyostelium discoideum*. *Science (Wash. DC)*. 236:1081–1086.

Mermall, V., J. G. McNally, and K. G. Miller. 1994. Transport of cytoplasmic particles catalysed by an unconventional myosin in living *Drosophila* embryos. *Nature (Lond.)*. 369:560–562.

Miller, K. G., C. M. Field, and B. M. Alberts. 1989. Actin-binding proteins from *Drosophila* embryos: a complex network of interacting proteins detected by F-actin affinity chromatography. *J. Cell Biol.* 109:2963–2975.

Minden, J. S., D. A. Agard, J. W. Sedat, and B. M. Alberts. 1989. Direct cell lineage analysis in *Drosophila melanogaster* by time-lapse three dimensional optical microscopy of living embryos. *J. Cell Biol.* 109:505–516.

Miyata, H., B. Bowers, and E. D. Korn. 1989. Plasma membrane association of *Acanthamoeba* myosin I. *J. Cell Biol.* 109:1519–1528.

Pasternak, C., J. A. Spudich, and E. L. Elson. 1989. Capping of surface receptors and concomitant cortical tension are generated by conventional myosin. *Nature (Lond.)*. 341:549–551.

Peters, D. J. M., D. A. Knecht, W. F. Loomis, A. D. Lozanne, J. Spudich, and P. J. M. V. Haastert. 1988. Signal transduction, chemotaxis, and cell aggregation in *Dictyostelium discoideum* cells without myosin heavy chain. *Dev. Biol.* 128:158–163.

Pollard, T. D., and J. A. Cooper. 1986. Actin and actin-binding proteins. A critical evaluation of mechanisms and functions. *Annu. Rev. Biochem.* 55:987–1035.

Pollard, T. D., S. K. Doberstein, and H. G. Zot. 1991. Myosin I. *Annu. Rev. Physiol.* 53:653–681.

Postner, M. A., K. G. Miller, and E. F. Wieschaus. 1992. Maternal effect mutations of the *sponge* locus affect actin cytoskeletal rearrangements in *Drosophila melanogaster* embryos. *J. Cell Biol.* 119:1205–1218.

Raff, J. W., and D. M. Glover. 1989. Centrosomes, and not nuclei, initiate pole cell formation in Drosophila embryos. *Cell*. 57:611–619.

Sullivan, W., J. S. Minden, and B. M. Alberts. 1990. Daughterless-abo-like, a *Drosophila* maternal-effect mutation that exhibits abnormal centrosome separation during late blastoderm division. *Development*. 110:311–323.

Sullivan, W., D. R. Daily, P. Fogarty, K. J. Yook and S. Pimpinelli. 1993*a*. Delays in anaphase initiation occur in individual nuclei of the syncytial *Drosophila* embryo. *Mol. Biol. Cell*. 4:885–896.

Sullivan, W., P. Fogarty, and W. Theurkauf. 1993*b*. Mutations affecting the cytoskeleton of syncytial *Drosophila* embryos. *Development*. 118:1245–1254.

Tan, J. L., S. Ravid, and J. A. Spudich. 1992. Control of nonmuscle myosins by phosphorylation. *Annu. Rev. Biochem.* 61:721–759.

Titus, M. A., D. Wessels, J. A. Spudich, and D. Soll. 1993. The unconventional myosin encoded by the *myoA* gene plays a role in *Dictyostelium* motility. *Mol. Biol. Cell*. 4:233–246.

Wagner, M. C., B. Barylko, and J. P. Albanesi. 1992. Tissue distribution and subcellular localization of mammalian myosin I. *J. Cell Biol.* 119:163–170.

Warn, R. M., L. Flegg, and A. Warn. 1987. An investigation of microtubule organization and functions in living *Drosophila* embryos by injection of fluorescently labeled antibody against tyrosinated a-tubulin. *J. Cell Biol.* 105: 1721–1730.

Weeds, A. 1982. Actin-binding proteins—regulators of cell architecture and motility. *Nature (Lond.)*. 296:811–816.

Wessels, D., D. R. Soll, D. Knecht, W. Loomis, A. D. Lozanne, and J. Spudich. 1988. Cell motility and chemotaxis in *Dictyostelium* amoebae lacking myosin heavy chain. *Dev. Biol.* 128:164–177.

Wessels, D., J. Murray, G. Jung, J. A. I. Hammer, and D. R. Soll. 1991. Myosin IB null mutants of *Dictyostelium* exhibit abnormalities in motility. *Cell Motil. Cytoskel.* 20:301–315.

Wolenski, J. S., S. M. Hayden, P. Forscher, and M. S. Mooseker. 1993. Calcium-calmodulin and regulation of brush border myosin-I MgATPase and mechanochemistry. *J. Cell Biol.* 122:613–621.

Yasuda, G. K., J. Baker, and G. Schubiger. 1991. Independent roles of centrosomes and DNA in organizing the *Drosophila* cytoskeleton. *Development*. 111:379–391.

Young, P. E., T. C. Pesacreta, and D. P. Kiehart. 1991. Dynamic changes in the distribution of cytoplasmic myosin during *Drosophila* embryogenesis. *Development*. 111:1–14.

Zalokar, M., and I. Erk. 1976. Division and migration of nuclei during early embryogenesis of *Drosophila melanogaster*. *J. Microsc. Biol. Cell*. 25:97–106.

Zot, H. G., S. K. Doberstein, and T. D. Pollard. 1992. Myosin-I moves actin filaments on a phospholipid substrate: implications for membrane targeting. *J. Cell Biol.* 116:367–376.